Interfacial Properties of Cyclic Hydrocarbons: A Monte Carlo Study

Jiří Janeček,[†] Hartmut Krienke,*[,‡] and Georg Schmeer[‡]

Physik Department, Technische Universitat München, 85748 Garching, Germany, and Institute of Physical and Theoretical Chemistry, University of Regensburg, 93040 Regensburg, Germany

Received: September 29, 2005; In Final Form: February 8, 2006

The Monte Carlo technique is used to study the vapor−liquid interface of cyclopentane, cyclohexane, and benzene. The OPLS and TraPPE potential fields are compared in the temperature range from 298.15 to 348.15 K (273.15−298.15 K for C_5H_{10}). A new method for the treatment of the long-range interactions in inhomogeneous simulations is used. When this new method is employed, the obtained values of saturated liquid density and of enthalpy of vaporization are equal to those obtained using the bulk isothermal−isobaric Monte Carlo technique. The values of surface tension become independent of the cutoff distance and they are significantly larger than those when only simple spherical truncation of intermolecular interactions is used.

1. Introduction

Hydrocarbons represent a class of organic compounds, which are frequently studied by molecular simulations. This is caused in the first place by their great industrial importance. Also more complex systems, in which the hydrophobic interactions play a significant role, can be modeled by hydrocarbons at a simplified level; many such systems are of use in enviromental, clinical, and biological applications.[1−4]

Since the 1970s, a series of potential energy models for hydrocarbons and their derivatives were developed. Almost all these models have some common attributes—they consider the molecule as a set of interaction sites (atoms or groups of atoms) and the interaction energy between the two molecules is given by the sum of interaction energies between all pairs of sites. The interaction between sites is then usually modeled as Lennard-Jones energy and—in the case of polar compounds—as a Coulombic interaction between partial charges located on the sites. The potential parameters are appointed by the functional type of the atom (group) only and do not depend on farther parts of the molecule. Thus, it is possible to simulate hundreds of substances with a set of parameters for only several tens of atoms (groups).

The Optimized Potential for Liquid Simulations (OPLS) is the first model with the above-mentioned features which was parametrized by molecular simulations.[5] The OPLS parameters were determined using the isothermal−isobaric Monte Carlo simulations (NPT MC) to obtain accurate values of enthalpies of vaporization and liquid densities at normal pressure and temperature. To describe the CH_n groups, the so-called united atom approach was used—these groups were modeled as one interaction site located at the carbon atom. This model—primarily parametrized for hydrocarbons only—was later extended to alcohols as well.[6]

To gain a better description at higher temperatures, Siepmann et al.[7] used the Gibbs Ensemble Monte Carlo technique (GEMC) to determine the vapor−liquid coexistence curves for several *n*-alkanes. Subsequently, a new potential field for hydrocarbons was developed, which offered a better agreement with experimental Vapor−Liquid Equilibrium (VLE) data in a broad range of temperatures;[8−10] this model is abbreviated as TraPPE (Transferable Potentials for Phase Equilibria). Later on, the parameters for alcohols, ethers, glycols, ketones, and aldehydes were determined,[11,12] and the version with an explicit description of hydrogen atoms was established.[13]

The parameters for the methylene group within the OPLS model were obtained by fitting to the liquid density and enthalpy of vaporization of cyclopentane, and they are designed for both—linear and cyclic—hydrocarbons. Through the use of these parameters in simulations of hexane, the parameters for the terminal methyl group were determined; these parameters for the CH_3 group employed in simulations of ethane do not give the correct results, and thus two different parameter sets for the methyl group are used in OPLS. In the case of TraPPE, the parameters for the CH_2 group were obtained by fitting to the VLE data of long alkanes. Neubauer et al.[14] have demonstrated that these interaction parameters cannot be directly transferred to cyclic alkanes as the constraints imposed by the cyclic structure affect the conformational equilibria and also the polarizability of the sites. They also found that the OPLS parameters for cyclohexane considerably overestimate the critical temperature and the liquid densities and suggested new parameter sets for cyclic hydrocarbons. Recently, the TraPPE parameters for the cyclic methylene group obtained from fitting to properties of cyclooctane were reported.[15] These parameters yield a satisfactory prediction of the coexistence curve of cyclohexane, but for cyclopentane, they work worse.

One way to study the VLE is the direct simulation of two coexisting phases in one box. The algorithm of this method is identical to that of standard NVT simulations, the only modification consists of the use of a box elongated in one direction and an appropriate decrease of the number density. At temperatures lower than the critical one, the system splits into two phases of different densities with the interface perpendicular to the elongated edge of the box to minimize the surface energy. This technique was used to study the vapor−liquid interfaces in various systems—Lennard-Jones fluid,[16] molten salts,[17] water,[18−20] aqueous solutions,[21,22] etc. This method can also be modified to study the liquid−liquid

* To whom correspondence should be addressed. E-mail: hartmut.krienke@chemie.uni-regensburg.de.
[†] Technische Universitat München.
[‡] University of Regensberg.

10.1021/jp055558d CCC: $33.50
Published on Web 03/11/2006

equilibria between two immiscible liquids.[23,24] The use of boxes with an interface in the GEMC represents also a powerful technique, which enables us to study the properties of the interface between vapor and a saturated solution of two immiscible liquids.[25−27]

Harris was the first, who performed molecular dynamics (MD) in this arrangement to study the structure of the free interface of alkane oligomers.[28] Later, similar systems were studied by Alejandre et al.[29] and Nicolas et al.[30] All these investigations were performed using the MD technique. It is well-known that the equilibrium properties—especially those of nonpolar systems—depend significantly on the form of the truncation of dispersion interactions and on the applied cutoff radius. In the case of the Lennard-Jones fluid, the differences between the values of the coexisting densities obtained by MD (where the truncation of forces is used) or MC (where the pair energy is truncated) can reach 10%; in the case of surface tension, this difference can be in the range up to 30%.[16] Because the parameters of both above-mentioned potential fields (OPLS and TraPPE) were obtained using bulk MC techniques and the long-range corrections to the energy were taken into account during these parametrizations, these two force fields will offer an adequate description of the VLE in inhomogeneous simulations only, when they are considered with included long-range corrections, as was nicely demonstrated in ref 31.

The Ewald summation technique for Coulombic interactions can be simply modified for inhomogeneous systems without any considerable increase in computational time.[32] For dispersion interactions, the extension of the simple approach used in bulk simulations is not straightforward, as this method assumes homogeneous density of the simulated system. In the case of water and aqueous solutions, the contribution from electrostatic forces is several orders higher than that from dispersion forces and the behavior of these systems is not affected by improper treatment or neglect of the long-range contributions from the dispersion interactions. Nevertheless, for most other polar liquids, both contributions are about of the same order and an adequate treatment of the long-range corrections of the truncated dispersion interactions is necessary to obtain a sufficiently accurate description of the phase equilibria.

Several approaches were suggested to treat the truncated dispersion interactions during inhomogeneous simulations. Guo et al.[33,34] suggested an approach based on the assumption of the local dependence of thermodynamic properties. Mecke et al.[35] have included the long-range corrections within MD simulation by adding an additive force contribution in the direction perpendicular to the interface. In the case of Lennard-Jones fluid, both methods give better results in comparison with simulations without any long-range corrections. Nevertheless, the obtained density profiles and the values of the surface tension show at higher temperatures a significant dependency on the cutoff radius. López-Lemus et al.[36,37] used the lattice sum technique for the dispersion energy. Despite that this method causes a strong increase in computational time (comparable with that caused by the inclusion of the Ewald summation), it seems to be more efficient than simulations with a very large cutoff distance, since smaller system sizes and numbers of particles are required. Lagüe et al.[38] presented a method for accounting the long-range terms in NPT ensembles which consists of applying an additional pressure. It is evaluated during the simulation from the difference of instantaneous pressure calculated on one hand at a given cutoff distance and on the other hand at a very large cutoff distance. As this method is restricted to the NPT ensemble, it is not suited to be directly used in the studies of the VLE. Recently, we have proposed a new method for treating the long-range corrections in systems with a planar interface.[39] In the case of Lennard-Jones particles, this method is working surprisingly well. For cutoff distances between 2.5σ and 5.0σ, this method gives identical density profiles and surface tension values for temperatures up to 0.95% of the critical temperature. The increase of computational time is only about 20% compared with simulations without any long-range corrections.

In this work, we apply this recent approach to molecular fluids. After a short explanation of the used approach, we present a comparison of the simulation results of the interfacial properties obtained for the two various potential fields with respect to the experimental values for three cyclic hydrocarbons.

2. Simulation Details

2.1. Potential Model. The configurational energy of a system composed of particles interacting via any interaction site model can be expressed as

$$U = \frac{1}{2}\sum_i \sum_{j\neq i} \sum_{\alpha\in i} \sum_{\beta\in j} u_{\alpha\beta}(r_{\alpha\beta}) + \sum_i U_i^{\text{intra}} \qquad (1)$$

where $u_{\alpha\beta}(r_{\alpha\beta})$ represents the interaction between sites α on molecule i and β on j, $r_{\alpha\beta}$ is the separation between these two sites, and U_i^{intra} stands for the intramolecular energy of molecule i. Within both models, OPLS and TraPPE, the interactions between sites are given by Lennard-Jones and Coulombic terms.

$$u_{\alpha\beta}(r_{\alpha\beta}) = 4\epsilon_{\alpha\beta}\left[\left(\frac{\sigma_{\alpha\beta}}{r_{\alpha\beta}}\right)^{12} - \left(\frac{\sigma_{\alpha\beta}}{r_{\alpha\beta}}\right)^{6}\right] + \frac{1}{4\pi\epsilon_o}\frac{q_\alpha q_\beta}{r_{\alpha\beta}} \qquad (2)$$

Values of the parameters $\sigma_{\alpha\alpha}$, $\epsilon_{\alpha\alpha}$, and q_α have been parametrized for a set of different functional groups. The parameters for unlike interactions are usually calculated using the Lorentz−Berthelot combining rules $\sigma_{\alpha\beta} = (\sigma_{\alpha\alpha} + \sigma_{\beta\beta})/2$ and $\epsilon_{\alpha\beta} = (\epsilon_{\alpha\alpha}\epsilon_{\beta\beta})^{1/2}$. The intramolecular energy, U_i^{intra}, is given by the interactions between distant sites in one molecule and by the torsion energy corresponding to the actual conformation and—eventually—by bond-length stretching and bending of bond angles (see refs 5 and 8).

Within this work, we used the united atom approach for all three studied compounds, which means that the nonpolar groups CH_3, CH_2, and CH are modeled as one site. The models with an explicit description of hydrogen sites offer slightly better results especially for aromatic compounds,[25] since they include their quadrupolar moment due to the charge distribution of different sites. Nevertheless, the improvement on the order of only several percent of the results is paid by a 2−3 times increase in the computational time.

To simulate the systems of flexible molecules entails several problems, which are not easy to solve. Moreover, the description of the flexibility makes the simulations considerably more time-consuming. Thus, we directed our attention to compounds, the molecules of which can be (more or less) considered to be rigid. Although the molecule of cyclopentane is not ideally planar, we modeled it as a planar rigid pentagon with the edge equal to the length of the C−C bond. The molecule of cyclohexane forms two stable conformations. While in the vapor phase, the chair conformation strongly dominates the boat conformation, in liquid, their mutual ratio is aligned to ca. 3:1.[40] Thus, we considered it to be composed only of the lowest energy chair conformation. The benzene molecule is modeled as a rigid planar hexagon.

TABLE 1: Parameters of OPLS and TraPPE Models

		OPLS	TraPPE
cycloalkanes	r_{C-C}	1.53 Å	1.54 Å
	α_{C-C-C}	112°	114°
	σ_{CH_2}	3.905 Å	3.89 Å
	ϵ_{CH_2}/k_B	59.4 K	51.0 K
benzene	r_{C-C}	1.40 Å	1.40 Å
	α_{C-C-C}	120°	120°
	σ_{CH}	3.75 Å	3.695 Å
	ϵ_{CH}/k_B	55.4 K	50.5 K

The values of the parameters for both sets used within this work are listed in Table 1. Compared with the "correct" OPLS force field, the only difference consists of neglecting the conformational equilibria in the case of cyclohexane. For cyclopentane and benzene, identical models were used by Jorgensen et al. to parametrize this force field.[5] The TraPPE parameters of the methylene group in cyclic hydrocarbons were obtained by fitting to the VLE data of cyclooctane. They perform quite well for larger cycloalkanes and worse for cyclopentane and cyclohexane.[15] This potential model also requires consideration of the harmonic bending of bond angles which can lead to further differences in all three cases.

2.2. Simulation Technique. To study the VLE, we performed the inhomogeneous NVT Monte Carlo simulations in a parallelepiped box. The program MCFLUID[41] modified for inhomogeneous systems was used. In the case of cyclopentane, the simulation box with the dimensions 35 × 35 × 210 Å contained 512 molecules. For benzene and cyclohexane, we took 343 molecules in a box with sizes 30 × 30 × 225 Å. The questions of simulation setup in inhomogeneous simulations have been intensively discussed.[16,42] The problems concerning the necessary number of particles and the form of truncation of intermolecular interactions can be reduced by a suitable treatment of the long-range corrections.[36,39] Recently, Orea et al. have found that new problems may arise from the choice of proper shape of the simulation box, even if the long-range corrections are treated adequately.[43] They have observed strong oscillations of the values of the surface tension of the Lennard-Jones fluid depending on the lateral dimension of the simulation box, which can reach more than 10%. This effect can be substantial in boxes with a lateral dimension smaller than 8σ. We have not performed detailed studies of this phenomenon in our systems, but to model the coexisting phases in an adequate way, we have chosen as a compromise sufficiently thick layers of both phases.

The initial configurations were prepared by bulk NPT MC simulations in parallelepiped boxes with identical lateral dimensions at the respective temperatures. To conserve the lateral dimension, the volume changes during these preparing NPT simulations were performed by dilatation and contraction of the z-axis only—instead of the commonly used spatially isotropic change of the volume. After an initial period of 5×10^4 MC cycles to stabilize the interface, three runs were performed, each of the length of 2.5×10^5 MC cycles. The translational and rotational displacements were adjusted to get the acceptance ratio between 0.3 and 0.5.

The recommended values of the cutoff distances—12.5 Å for OPLS and 14.0 Å for TraPPE—were used within all simulations. The molecular truncation of the intermolecular energy was applied, which means that the truncation was based simply on the center−center separation and was not explicitly taken into account for each pair of sites. Use of the site−site based cutoff would be more consistent with the suggested treatment of long-range corrections; nevertheless, the molecular based cutoff was already implemented in our program and it makes the simulation slightly faster compared with site−site cutoff. Moreover, for small, rigid molecules, the difference between these two approaches should not be significant.

According to our recent approach, the long-range correction term to the energy of a molecule i of component a depends on the z-coordinate of this molecule and on the course of the density profiles of all components.[39] The general relation for an $\mathcal{N}_c$-component system can be written as

$$\mathcal{U}_{i,a}^{\mathrm{lrc}}(z_i) = \sum_k \sum_{b=1}^{\mathcal{N}_c} \rho_b(z_k) w^{ab}(|z_k - z_i|)\Delta z \tag{3}$$

where the first summation runs over all strips into which the box is divided, while the second one runs over all components; Δz is the thickness of one strip, $\rho_b(z_k)$ is the local density of component b in strip k, and the function $w^{ab}(\xi)$ has the following form

$$w^{ab}(\xi) = \begin{cases} 4\pi \sum_{\alpha=1}^{n_a^s} \sum_{\beta=1}^{n_b^s} \epsilon_{\alpha\beta}\sigma_{\alpha\beta}^2 \left[\frac{1}{5}\left(\frac{\sigma_{\alpha\beta}}{R_c}\right)^{10} - \frac{1}{2}\left(\frac{\sigma_{\alpha\beta}}{R_c}\right)^{4}\right] & \xi \le R_c \\ 4\pi \sum_{\alpha=1}^{n_a^s} \sum_{\beta=1}^{n_b^s} \epsilon_{\alpha\beta}\sigma_{\alpha\beta}^2 \left[\frac{1}{5}\left(\frac{\sigma_{\alpha\beta}}{\xi}\right)^{10} - \frac{1}{2}\left(\frac{\sigma_{\alpha\beta}}{\xi}\right)^{4}\right] & \xi > R_c \end{cases} \tag{4}$$

where α runs over n_a^s sites of component a and β runs over n_b^s sites of b. This can be also expressed in an alternative way, which is more convenient to the site−site cutoff

$$\mathcal{U}_{i,a}^{\mathrm{lrc}}(z_i) = \sum_k \sum_{\alpha=1}^{n_a^s} \sum_{b=1}^{\mathcal{N}_c} \sum_{\beta=1}^{n_b^s} \rho_\beta(z_k) w^{\alpha\beta}(|z_k - z_i|)\Delta z \tag{5}$$

where now $\rho_\beta(z_k)$ is the density profile of site β and

$$w^{\alpha\beta}(\xi) = \begin{cases} 4\pi\epsilon_{\alpha\beta}\sigma_{\alpha\beta}^2 \left[\frac{1}{5}\left(\frac{\sigma_{\alpha\beta}}{R_c}\right)^{10} - \frac{1}{2}\left(\frac{\sigma_{\alpha\beta}}{R_c}\right)^{4}\right] & \xi \le R_c \\ 4\pi\epsilon_{\alpha\beta}\sigma_{\alpha\beta}^2 \left[\frac{1}{5}\left(\frac{\sigma_{\alpha\beta}}{\xi}\right)^{10} - \frac{1}{2}\left(\frac{\sigma_{\alpha\beta}}{\xi}\right)^{4}\right] & \xi > R_c \end{cases} \tag{6}$$

When the long-range corrections to the energy of the moved molecule are applied in one of these ways in every MC step, the behavior of the system is considerably more closely related to the behavior of a system with nontruncated interactions.

The density profiles for sites and molecular centers along the z-axis were recorded in strips of thickness 0.25 Å after every 10 MC cycles. With the same frequency, the energy felt by every molecule was calculated and stored as a function of its z-coordinate. Such "energy" profiles enable us to determine the excess internal energy of the coexisting phases. One can then simply evaluate the molar enthalpy of vaporization H^{vap} using the formula

$$\frac{H^{\mathrm{vap}}}{RT} = \frac{U_g - U_l}{RT} + \frac{P^o(v_g - v_l)}{RT} \tag{7}$$

where the subscripts g and l refer to the gaseous and liquid phases, U is the excess internal energy per one mole, v are the molar volumes of the bulk phases, P^o is the vapor pressure at temperature T, and R is the molar gas constant. The molar

volumes are obtained from the density profiles, and also the vapor pressure can be estimated from the simulations. As our simulations were performed at low temperatures, we were allowed to replace the second term simply by the compressibility factor of the ideal gas.

The projection of the main symmetry axis onto the *z*-axis of the box was also measured for all molecules, and their distribution in particular strips was also stored every 10 MC cycles. Since the main axis of symmetry is perpendicular to the molecular plane in all three cases, this quantity also corresponds to the distribution of the angle between the normal vector and *z*-axis. A similar orientational order parameter was previously investigated for the vapor−liquid interfaces of ethane, *n*-butane, and *n*-hexane.[44]

The surface tension was measured as the difference of the diagonal components of the configurational part of the virial tensor

$$\gamma = \frac{1}{2S}\left[2\Pi_{zz} - (\Pi_{xx} + \Pi_{yy})\right] \tag{8}$$

where S is the surface area of the interface, and the components of the virial tensor are given as

$$\Pi_{\mu\nu} = \langle \sum_{a=1}^{\mathcal{N}_c} \sum_{i=1}^{N_a} r_i^{\mu} F_i^{\nu} \rangle \tag{9}$$

Here, i is running over all N_a molecules of component a, $\langle ... \rangle$ stands for the canonical average, and μ and ν stand for the x, y, and z components of the position vector $\mathbf{r}$ of particle i or of the force $\mathbf{F}$ acting on this particle.

Following again the approach of ref 39, we can express the components of the virial tensor as a sum of direct interactions and of the long-range contribution

$$\Pi_{\mu\nu} = \langle \sum_{a=1}^{\mathcal{N}_c} \sum_{i=1}^{N_a} r_i^{\mu} \hat{F}_i^{\nu} \rangle + \sum_{a=1}^{\mathcal{N}_c} \sum_{i=1}^{N_a} \Delta\Pi_{\mu\nu}^{i,a,\mathrm{lrc}}(z_i) \tag{10}$$

where $\hat{\mathbf{F}}_\mathbf{i}$ is the direct force acting on particle i by all particles inside the cutoff sphere; the summations again go over all N_a particles of all species a. The correction part to the $\mu\nu$ component of Π due to the forces acting on molecule i from the volume outside the cutoff sphere can be expressed in a similar way as in the case of the energy

$$\Delta\Pi_{\mu\nu}^{i,a,\mathrm{lrc}}(z_i) = \sum_{k} \sum_{b=1}^{\mathcal{N}_c} \rho_b(z_k) \pi_{\mu\nu}^{ab}(z_k - z_i) \Delta z \tag{11}$$

The generalized relations for $\pi_{xx}^{ab}(\xi)$, $\pi_{yy}^{ab}(\xi)$, and $\pi_{zz}^{ab}(\xi)$ for a pair of different components can be written as

$$\pi_{xx}^{ab}(\xi) = \pi_{yy}^{ab}(\xi) = \begin{cases} 2\pi \sum_{\alpha=1}^{n_a^s} \sum_{\beta=1}^{n_b^s} \epsilon_{\alpha\beta} \left[\frac{6R_c^2 - 5\xi^2}{5} \left(\frac{\sigma_{\alpha\beta}}{R_c}\right)^{12} - \frac{6R_c^2 - 5\xi^2}{2} \left(\frac{\sigma_{\alpha\beta}}{R_c}\right)^{6} \right] & \xi \le R_c \\ 2\pi \sum_{\alpha=1}^{n_a^s} \sum_{\beta=1}^{n_b^s} \epsilon_{\alpha\beta} \left[\frac{\xi^2}{5} \left(\frac{\sigma_{\alpha\beta}}{\xi}\right)^{12} - \frac{\xi^2}{2} \left(\frac{\sigma_{\alpha\beta}}{\xi}\right)^{6} \right] & \xi > R_c \end{cases} \tag{12}$$

and

$$\pi_{zz}^{ab}(\xi) = \begin{cases} 4\pi \sum_{\alpha=1}^{n_a^s} \sum_{\beta=1}^{n_b^s} \epsilon_{\alpha\beta} \xi^2 \left[\left(\frac{\sigma_{\alpha\beta}}{R_c}\right)^{12} - \left(\frac{\sigma_{\alpha\beta}}{R_c}\right)^{6} \right] & \xi \le R_c \\ 4\pi \sum_{\alpha=1}^{n_a^s} \sum_{\beta=1}^{n_b^s} \epsilon_{\alpha\beta} \xi^2 \left[\left(\frac{\sigma_{\alpha\beta}}{\xi}\right)^{12} - \left(\frac{\sigma_{\alpha\beta}}{\xi}\right)^{6} \right] & \xi > R_c \end{cases} \tag{13}$$

The components of the virial tensor were measured after every 10 MC cycles as well. The direct part of the profiles of normal and transversal pressure were calculated in the standard way,[16] and the contributions from the lrc's was added at every measurement for every molecule occurring at the given strip.

We have also performed bulk isothermal−isobaric Monte Carlo (NPT MC) simulations for all studied systems. These simulations give the values directly of heat of vaporization (assuming ideal behavior of the vapor phase) and liquid densities, which can then be compared with results of inhomogeneous simulations. As we model the studied hydrocarbons on a slightly simplified level, we cannot expect perfect agreement between our results and the experimental values; however, the results of inhomogeneous simulations should be consistent with other techniques (in this case NPT MC), if the long-range corrections are treated adequately. These NPT simulations were performed using parallelepiped boxes with the same lateral dimensions as we used for the inhomogeneous simulations, and the volume changes were performed by a dilatation/contraction of the *z*-axis only instead of the commonly used spatially isotropic change of the volume of a cubic box. We were then allowed to use the final configuration from these simulations as the starting configurations for our inhomogeneous simulations of the VLE. Recently, it was found that the use of noncubic boxes can cause strong anisotropy of the pressure tensor even for homogeneous systems.[45] We have thus repeated our NPT simulation also in cubic boxes.

In the case of cyclopentane, the system again contained 512 molecules, those for benzene and cyclohexane contained 343 molecules. The simulations in the cubic boxes were started from simple cubic lattices with approximately experimental density; those in the parallelepiped boxes were started from orthogonal lattices with such a value of *z*-elongation that the number density of these lattices was again equal to the experimental number density of the corresponding liquids. After 5×10^6 MC steps at constant volume, we performed one relaxation NPT run. The enthalpies of vaporization and liquid densities were obtained from 25 000 records during simulations, which are 2.5×10^5 MC cycles long. The translational and rotational movements of molecules were adjusted to give a 0.3−0.5 acceptance ratio, and the maximal volume dilatation was set to give ca. 20% accepted changes. At every temperature, three independent runs were performed.

Within the NPT simulations, the molecular cutoff was again applied. The long-range corrections felt by one molecule of component a are given by the standard formula

$$u_{\mathrm{lrc}}^{a} = \sum_{\alpha=1}^{n_a^s} \sum_{b=1}^{\mathcal{N}_c} \sum_{\beta=1}^{n_b^s} 4\pi\rho_b \int_{R_c}^{\infty} r^2 u_{\alpha\beta}(r)\, \mathrm{d}r = \sum_{\alpha=1}^{n_a^s} \sum_{b=1}^{\mathcal{N}_c} \sum_{\beta=1}^{n_b^s} 16\pi\rho_b \epsilon_{\alpha\beta} \left(\frac{\sigma_{\alpha\beta}^{12}}{9R_c^9} - \frac{\sigma_{\alpha\beta}^{6}}{3R_c^3} \right) \tag{14}$$

where all symbols should have the same meaning as in the relations for inhomogeneous systems. In the case of a one-

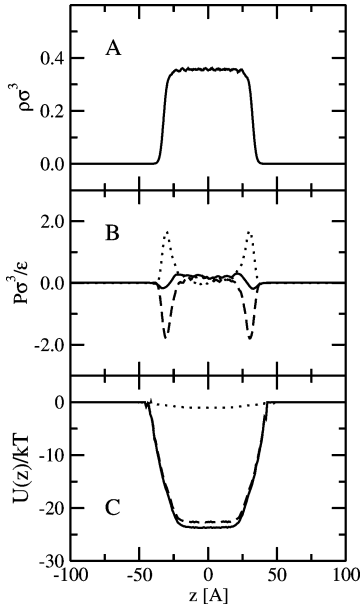

Figure 1. (A) Density profile for OPLS cyclopentane at 273.15 K. (B) Profile of normal (solid line) and transversal (dashed line) components of the pressure. The dotted line shows their difference; the integration of the area under this curve is an alternative approach to obtaining the surface tension. (C) The energy profiles felt by one molecule. The meaning of the different energy profiles is explained in the text.

component system, this relation is reduced to

$$u_{\mathrm{lrc}}^{a} = \sum_{\alpha=1}^{n^s} \sum_{\beta=1}^{n^s} 16\pi\rho\epsilon_{\alpha\beta}\left(\frac{\sigma_{\alpha\beta}^{12}}{9R_c^9} - \frac{\sigma_{\alpha\beta}^{6}}{3R_c^3}\right) \qquad (15)$$

With respect to the dependence of the lrc energy on the density this term should not be omitted within the acceptance/rejection criterion for the changes of the volume of the box.

3. Results

A representative density profile of sites of OPLS cyclopentane at 273.15 K is shown in Figure 1A. At this temperature, the particle density in the vapor phase is too small to be calculated accurately at the simulations. Due to this reason, we were not able to determine the values of the vapor pressure of the three studied compounds.

In Figure 1B, the profiles of normal and transversal (tangential) pressure and their difference are shown. One can see that the profile of the normal component of the pressure (solid line) is not strictly constant through the interface. Nevertheless, the small difference between the average values in the two bulk phases as the wavelike structure at the interfaces as well do not indicate any mechanical instability of the system but are a consequence of the used long-range corrections of truncated interactions.

Similar effects were also observed in simulations of two-site particles.[46] The peaks at the interfaces in the course of the transversal pressure profile (dashed line) are responsible for the surface tension, and they are considerably larger than the small offset in bulk values of the normal pressure. The integration of the difference of normal and transversal components (dotted curve) is an alternative way to evaluate the surface tension (see, e.g., ref 16), which should lead to identical results as the direct method.

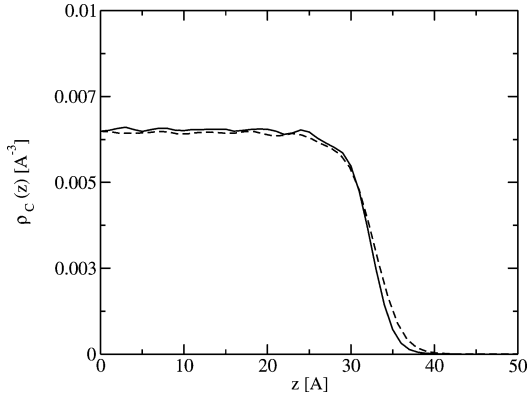

Figure 2. Influence of long-range corrections to the shape of the interface. The dashed line is the density profile of OPLS cyclopentane at 273.15 K when no lrc's are considered while the solid one is with included lrc's.

TABLE 2: Heat of Vaporization, Density of Liquid Phase, Surface Tension, and Thickness of the Interface for OPLS Cyclopentane at 273.15 K Obtained Using Various Simulation Techniques

	VLE[a]	VLE+ LRC[a]	NPT-cub[b]	NPT-par[b]
ΔH^{vap}/(kJ/mol)	27.7	29.2	29.22	29.20
ρ_{liq}/(kg/m^3)	751	762	763	762
γ/(mN/m)	23.4	31.1		
d_{10-90}/Å	7.4	6.2		
$Z_{xx}{}^c$			-0.96 ± 0.05	-1.12 ± 0.06
$Z_{yy}{}^c$			-0.97 ± 0.04	-1.09 ± 0.05
$Z_{zz}{}^c$			-0.96 ± 0.05	-0.96 ± 0.07

[a] VLE means inhomogeneous simulations without any long-range corrections. VLE + LRC means inhomogeneous simulations with the above-described approach. [b] NPT-cub and NPT-par are the bulk NPT MC simulations in cubic and parallelepiped boxes, respectively. [c] The last three rows show the configurational part of the components of the compressibility factor $Z_{\mu\mu} = \prod_{\mu\mu}/(\rho KT)$.

The profile of the energy felt by one molecule is shown in Figure 1C. The solid line represents the interaction energy with included long-range corrections, while the dashed one represents the direct part due to interactions with other molecules inside the cutoff sphere. One can see that the lrc's (dotted line) in this case cover about 5% of the excess internal energy of the liquid phase. The larger recommended cutoff distance for the TraPPE model slightly lowers this effect; nonetheless, the adequate treatment of the long-range contributions remains important. We note only that the excess internal energy per one molecule is only half of the value at the plateaus, as by the construction of the energy profile every molecule is counted twice.

To demonstrate the influence of the included long-range corrections in the direct VLE simulations, we performed runs for the OPLS cyclopentane at $T = 273.15$ K with and without the lrc's. The corresponding density profiles are plotted in Figure 2. A broadening of the interface and a small decay of the liquid density appears when the lrc's are not involved (dashed line). The corresponding values of the heat of vaporization, liquid density, thickness of the interface, and the surface tension are listed in Table 2. For the enthalpy of vaporization and the liquid density, the values obtained from bulk NPT simulations are reported as well; the column NPT-cub shows the results obtained in a cubic box while NPT-par means results from the parallelepiped box. In the last three rows of this table, the components of the pressure tensor obtained in bulk NPT simulations in the two different boxes are compared; these quantities are reported as the configurational part of the compressibility factor. One can see that the omission of the long-range interactions leads

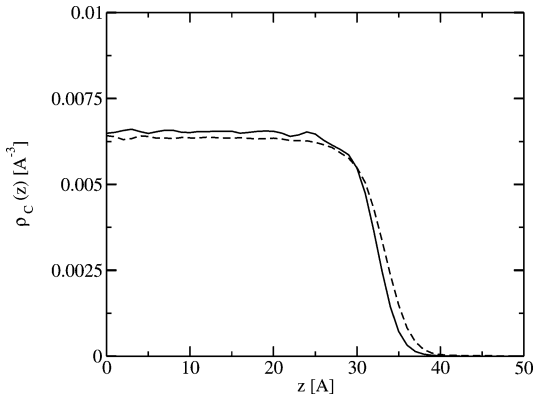

Figure 3. Effect of temperature on the density profiles. The solid curve represents the result for OPLS cyclopentane at 273.15 K; the dashed one represents that at 298.15 K.

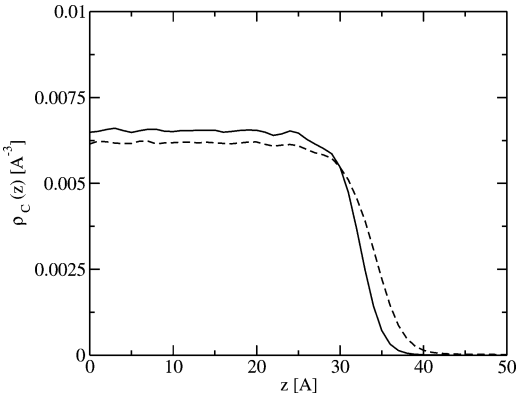

Figure 4. Difference between OPLS (solid line) and TraPPE (dashed line) density profiles for cyclopentane at 273.15 K.

to a decay of the liquid density, the enthalpy of vaporization, and the surface tension. On the other hand, there is a good agreement between the bulk properties obtained from the inhomogeneous simulations with included long-range corrections and from the bulk NPT simulations. Although the shape of the box considerably influences the isotropy of the pressure tensor, the values of the bulk properties at the studied conditions are identical for the cubic box as for the parallelepiped one as well. A similar effect was observed also by González-Melchor et al.[45] in their study of a Lennard-Jones fluid.

Figure 3 shows the influence of temperature on the density profile. Both curves correspond to OPLS cyclopentane; the solid line is at 273.15 K and the dashed one at 298.15 K. The difference between OPLS and TraPPE potentials for cyclopentane is shown in Figure 4. The main difference between these two models consists of the parameter ϵ, which is within the TraPPE model approximately 85% of the OPLS value. This is comparable with a change in temperature from 273.15 to 318 K taking the OPLS model (compare with Figure 3).

In Figure 5, three distributions of the cosinus of the angle between the normal unit vector and the *z*-axis, $\mathbf{n}\cdot\mathbf{e_z} = \cos\theta_{n,z}$, are plotted for OPLS cyclopentane at $T = 273.15$ K. In the inset in the right top corner the corresponding density profile is shown, in which the three vertical lines mark the positions to which the distributions correspond. The solid line represents such a distribution in the bulk liquid where it must be uniform. The dashed curve is the distribution at that strip, where the density is equal to 90% of the bulk value, while the dotted one is in a strip with a density of 10% of the bulk value. The dash−dotted line shows, for comparison, such a distribution for water, taken in the middle of the vapor−liquid interface (from ref 20).

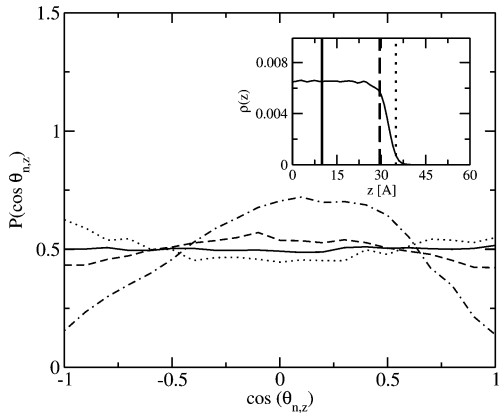

Figure 5. Distributions of cos $\theta_{n,z}$ for cyclopentane (OPLS model, 273.15 K): solid line, bulk liquid; dashed line, strip with $\rho(z) = 0.9\rho^{bulk}$; dotted line, strip with $\rho(z) = 0.1\rho^{bulk}$. The inset indicates the positions where the distributions were taken (the type of vertical lines in this plot corresponds to that in the main figure). The dot−dashed line shows the analogous distribution for water.

TABLE 3: Liquid Densities for Cyclopentane, Cyclohexane, and Benzene Obtained with OPLS and TraPPE Models Using Inhomogeneous MC Simulations (VLE) and Bulk NPT Simulations in a Cubic Box (NPT) (ρ in kg/m^3)

	OPLS		TraPPE		
T/K	NPT	VLE	NPT	VLE	exp
		cyclopentane			
273.15	763 ± 1	762 ± 2	721 ± 1	722 ± 2	764.8
298.15	740 ± 1	742 ± 2	693 ± 2	694 ± 2	740.4
		cyclohexane			
298.15	805 ± 1	804 ± 2	758 ± 1	760 ± 1	773.9
323.15	784 ± 2	785 ± 2	732 ± 2	734 ± 2	749.9
348.15	765 ± 1	765 ± 3	707 ± 1	710 ± 2	724.9
		benzene			
298.15	871 ± 2	869 ± 2	866 ± 1	864 ± 2	882.9
323.15	849 ± 2	849 ± 2	839 ± 1	837 ± 2	856.4
348.15	827 ± 2	829 ± 2	812 ± 2	815 ± 3	828.7

TABLE 4: Enthalpies of Vaporization for Cyclopentane, Cyclohexane, and Benzene Obtained with OPLS and TraPPE Models Using Different Simulation Techniques (H^{vap} in kJ/mol)

	OPLS		TraPPE		
T/K	NPT	VLE	NPT	VLE	exp
		cyclopentane			
273.15	29.22 ± 0.02	29.2 ± 0.1	23.33 ± 0.05	23.4 ± 0.1	29.7
298.15	28.29 ± 0.04	28.4 ± 0.1	22.46 ± 0.05	22.5 ± 0.1	28.4
		cyclohexane			
298.15	35.21 ± 0.05	35.1 ± 0.1	28.00 ± 0.07	28.1 ± 0.1	33.9
323.15	34.20 ± 0.03	34.3 ± 0.1	27.01 ± 0.05	27.1 ± 0.1	31.3
348.15	33.27 ± 0.05	33.2 ± 0.1	26.06 ± 0.05	26.3 ± 0.1	30.5
		benzene			
298.15	34.59 ± 0.05	34.5 ± 0.1	29.86 ± 0.05	29.8 ± 0.1	33.4
323.15	33.63 ± 0.05	33.7 ± 0.1	28.88 ± 0.05	28.8 ± 0.1	32.4
348.15	32.71 ± 0.05	32.8 ± 0.1	27.97 ± 0.05	27.9 ± 0.1	31.3

Regarding the two distributions in the interfacial region of cyclopentane, it is difficult to draw an unambiguous conclusion. They may demonstrate the smaller disposition of the outermost molecules to lie parallel to the interface. Nevertheless, this effect is considerably less obvious compared to the very perspicuous orientational effects in the water interface. For open chain alkanes, Harris[28] observed a small but undeniable lowering of the occurrence of CH_3 groups in the interface, which is caused by a slightly higher value of the ϵ parameter for the CH_3 group within the OPLS model. In contradiction to water and chain

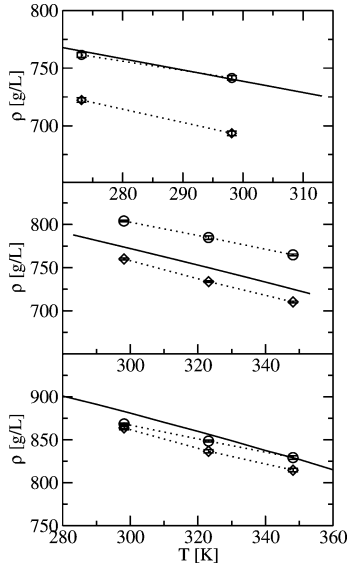

Figure 6. Liquid densities of the systems studied with NPT MC: circles, OPLS model; diamonds, TraPPE model; solid line, experimental data. (The inserts in the symbols show the error bars.) The upper part represents the results for cyclopentane, the middle one those for cyclohexane, and the lower one those for benzene.

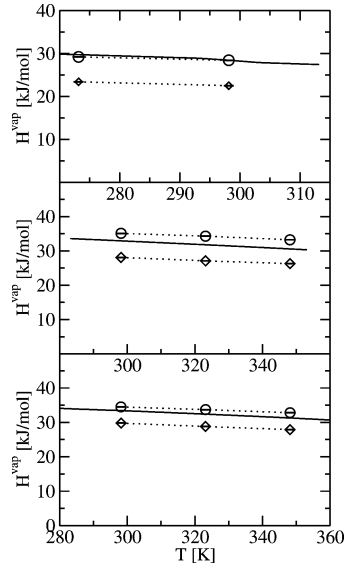

Figure 7. Enthalpies of vaporization of the systems studied with NPT MC: circles, OPLS model; diamonds, TraPPE model; solid line, experimental data. The upper part represents the results for cyclopentane, the middle one those for cyclohexane, and the lower one those for benzene.

alkanes, there is no energetic drive for any preferential orientation in our systems as all interaction sites are equivalent.

The values of the liquid densities are tabulated in Table 3. One can see that the values obtained using the NPT simulations are in all cases within the experimental errors identical with those obtained from inhomogeneous simulations. The same is also true for the values of heat of vaporization which are listed in Table 4. Again there is a very good agreement between the results of bulk NPT simulations in a cubic box and those of inhomogeneous simulations with involved long-range corrections. These results are shown in Figures 6 and 7 in the order: cyclopentane (top), cyclohexane (middle), benzene (bottom). In both figures, the circles represent the OPLS results, while the diamonds show those of the TraPPE model and the solid lines represent the experimental data.[47] One can observe a considerable difference between the two sets of simulation results for cyclopentane and cyclohexane. In the case of liquid densities, the difference is up to 10%, while for the enthalpy of vaporization it can reach 20%.

TABLE 5: Surface Tension and 10−90 Thickness Values for Simulated Systems (see Figure 5 and the text for explanation)

	d_{10-90}/Å		γ/(mN/m)		
T/K	OPLS	TraPPE	OPLS	TraPPE	exp
			cyclopentane		
273.15	6.2	8.2	31.1 ± 1.5	20.2 ± 0.6	
286.65	6.6	8.9	28.9 ± 0.8	18.3 ± 0.8	23.3
298.15	7.2	9.1	28.0 ± 1.2	16.8 ± 0.8	
			cyclohexane		
298.15	5.7	6.8	32.1 ± 1.5	22.1 ± 0.9	24.35
323.15	6.6	8.5	29.5 ± 1.8	19.3 ± 0.5	21.35
348.15	7.2	9.9	26.3 ± 0.6	15.9 ± 0.7	18.35
			benzene		
298.15	5.6	6.5	37.1 ± 2.0	30.1 ± 1.0	28.18
323.15	6.3	7.3	35.5 ± 2.0	25.7 ± 0.7	24.88
348.15	7.5	8.7	30.6 ± 1.0	22.1 ± 1.0	21.8

In Table 5, we present the values of surface tensions and 10−90 thicknesses obtained by direct VLE simulations with lrc's. The values of surface tensions are compared with the experimental data in Figure 8; the meaning of the lines and symbols is the same as that in Figures 6 and 7 with the exception of cyclopentane, where the single experimental value is shown as a square. One can see that the OPLS model overestimates the surface tension by 20−50%. This is in accordance with the results of Harris,[28] who found for liquid decane and eicosane a roughly good agreement between the directly calculated part of the surface tension via MC simulations and the experimental value. After the inclusion of the long-range correction to the calculation of the surface tension, the resulting values were also about 30% higher compared with the experimental values. Similar observations can also be found in the work of Nicolas and Smit.[30] In the case of the TraPPE potential, there is a good agreement between experimental and simulated values for benzene. For the two saturated hydrocarbons, the simulation results are lower compared with the experimental data. If the

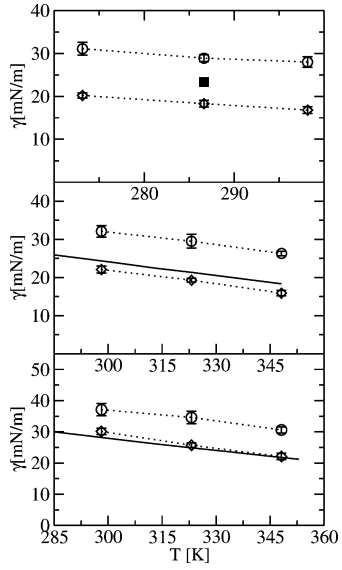

Figure 8. Surface tensions of the systems studied with NPT MC: circles, OPLS model; diamonds, TraPPE model; solid lines, experimental data. The upper part represents the results for cyclopentane with one experimental value (square). The middle part shows the results for cyclohexane and the lower part those for benzene.

flexibility of the molecules of these two compounds is considered, then we can suppose some increase of the simulated values of the liquid densities and also of the surface tensions. As we can guess from the figures and critical data reported in ref 15, the increase in the density is not too significant; the influence of neglected flexibility on the surface tension will probably be more remarkable. For short, linear alkanes, it was observed that the TraPPE parameters also slightly overestimate the values of the surface tension but to a considerably smaller extent.[44]

4. Conclusion

Monte Carlo simulations were performed to investigate the vapor−liquid interfacial properties for three cyclic hydrocarbons (cyclopentane, cyclohexane, and benzene) using two different force fields.

In the case of the OPLS potential model, a good agreement in the values of the heat of vaporization and the liquid densities was found for cyclopentane and benzene; this is a consequence of the fact that these two compounds were used to evaluate the σ and ϵ parameters for CH_2 and aromatic CH groups. For cyclohexane, our results are influenced by the neglected flexibility. Nevertheless, we dare to conclude that the OPLS model for cyclohexane considerably overestimates the liquid density and the heat of vaporization. For all three compounds, the OPLS model also considerably overestimates the values of the surface tension.

On first view, the comparison with experimental data in the case of the TraPPE model is slightly worse. Nevertheless, the deviations for cyclopentane and cyclohexane are probably caused by different flexibilities of their smaller rings (compared with cyclooctane for which the values of parameters were obtained). In the case of benzene, there is a remarkably good agreement of the values of the surface tension.

Acknowledgment. The stay of J.J. in Regensburg was supported by the Deutsche Forschungsgemeinschaft (Grant SCHM 605/5-3). We thank also Prof. Werner Kunz for additional support.

References and Notes

(1) Jorgensen, W. L.; Gao, J.; Ravimonah, C. *J. Phys. Chem.* **1985**, *89*, 3470.
(2) Jorgensen, W. L.; Duffy, E. M. *Bioorg. Med. Chem. Lett.* **2000**, *10*, 1155.
(3) Jedlovszky, P.; Mezei, M. *J. Chem. Phys.* **1999**, *111*, 10770.
(4) Jedlovszky, P.; Varga, I.; Gilányi, T. *J. Chem. Phys.* **2003**, *119*, 1731.
(5) Jorgensen, W. L.; Madura, J. D.; Swenson, C. J. *J. Am. Chem. Soc.* **1984**, *106*, 6638.
(6) Jorgensen, W. L. *J. Phys. Chem.* **1986**, *90*, 1276.
(7) Siepmann, J. I.; Karaborni, S.; Smit, B. *J. Am. Chem. Soc.* **1993**, *115*, 6454.
(8) Martin, M. G.; Siepmann, J. I. *J. Phys. Chem. B* **1998**, *102*, 2569.
(9) Martin, M. G.; Siepmann, J. I. *J. Phys. Chem. B* **1999**, *103*, 4508.
(10) Wick, C. D.; Martin, M. G.; Siepmann, J. I. *J. Phys. Chem. B* **2000**, *104*, 8008.
(11) Chen, B.; Potoff, J. J.; Siepmann, J. I. *J. Phys. Chem. B* **2001**, *105*, 3093.
(12) Stubbs, J. M.; Potoff, J. J.; Siepmann, J. I. *J. Phys. Chem. B* **2004**, *108*, 17596.
(13) Chen, B.; Siepmann, J. I. *J. Phys. Chem. B* **1999**, *103*, 5370.
(14) Neubauer, B.; Boutin, A.; Tavitian, B.; Fuchs, A. H. *Mol. Phys.* **1999**, *97*, 769.
(15) Lee, J.-S.; Wick, C. D.; Stubbs, J. M.; Siepmann, J. I. *Mol. Phys.* **2005**, *103*, 99.
(16) Trokhymchuk, A.; Alejandre, J. *J. Chem. Phys.* **1999**, *111*, 8510.
(17) Aguado, A.; Wilson, M.; Madden, P. A. *J. Chem. Phys.* **2001**, *115*, 8603.
(18) Wilson, M. A.; Pohorille, A.; Pratt, L. R. *J. Phys. Chem.* **1987**, *91*, 4873.
(19) Alejandre, J.; Tildesley, D. J.; Chapela, G. A. *J. Chem. Phys.* **1994**, *102*, 4574.
(20) Taylor, R. S.; Dang, L. X.; Garrett, B. C. *J. Phys. Chem.* **1996**, *100*, 11720.
(21) Jungwirth, P.; Tobias, D. J. *J. Phys. Chem. B* **2001**, *105*, 10468.
(22) Dang, L. X.; Chang, T.-M. *J. Phys. Chem B* **2002**, *106*, 235.
(23) Zhang, Y.; Feller, S. E.; Brooks, B. R.; Pastor, R. W. *J. Chem. Phys.* **1995**, *103*, 10252.
(24) Nicolas, J. P.; de Souza, N. R. *J. Chem. Phys.* **2004**, *120*, 2464.
(25) Wick, C. D.; Martin, M. G.; Siepmann, J. I.; Schure, M. R. *Int. J. Thermophys.* **2001**, *22*, 111.
(26) Wick, C. D.; Siepmann, J. I.; Schure, M. R. *Anal. Chem.* **2002**, *74*, 3518.
(27) Chen, B.; Siepmann, J. I.; Klein, M. L. *J. Am. Chem. Soc.* **2002**, *124*, 12232.
(28) Harris, J. G. *J. Phys. Chem.* **1992**, *96*, 5077.
(29) Alejandre, J.; Tildesley, D. J.; Chapela, G. A. *Mol. Phys.* **1995**, *85*, 651.
(30) Nicolas, J. P.; Smit, B. *Mol. Phys.* **2002**, *100*, 2471.
(31) Goujon, F.; Malfreyt, P.; Simon, J.-M.; Boutin, A.; Rousseau, B.; Fuchs, A. H. *J. Chem. Phys.* **2004**, *121*, 12559.
(32) Yeh, I.-C.; Berkowitz, M. L. *J. Chem. Phys.* **1999**, *111*, 3155.
(33) Guo, M.; Lu, B. C.-Y. *J. Chem. Phys.* **1997**, *106*, 3688.
(34) Guo, M.; Peng, D.-Y.; Lu, B. C.-Y. *Fluid Phase Equilib.* **1997**, *130*, 19.
(35) Mecke, M.; Winkelmann, J.; Fischer, J. *J. Chem. Phys.* **1997**, *107*, 9264.
(36) López-Lemus, J.; Alejandre, J. *Mol. Phys.* **2002**, *100*, 2983.
(37) López-Lemus, J.; Alejandre, J. *Mol. Phys.* **2003**, *101*, 743.
(38) Lagüe, P.; Pastor, R. W.; Brooks, B. R. *J. Phys. Chem. B* **2004**, *108*, 363.
(39) Janeček, J. *J. Phys. Chem. B*, in press.
(40) Harris, J. G.; Stillinger, F. H. *J. Chem. Phys.* **1991**, *95*, 5953.
(41) Fischer, R. Ph.D. Thesis, Uni Regensburg, Regensberg, Germany, 1998.
(42) Holcomb, C. D.; Clancy, P.; Zollweg, J. A. *Mol. Phys.* **1993**, *78*, 437.
(43) Orea, P.; López-Lemus, J.; Alejandre, J. *J. Chem. Phys.* **2005**, *123*, 114702.
(44) Chen, B.; Siepmann, J. I.; Oh, K. J.; Klein, M. L. *J. Chem. Phys.* **2002**, *116*, 4317.
(45) Gonzáles-Melchor, M.; Orea, P.; López-Lemus, J.; Bresme, F.; Alejandre, J. *J. Chem. Phys.* **2005**, *122*, 94503.
(46) Duque, D.; Vega, L. F. *J. Chem. Phys.* **2004**, *121*, 8611.
(47) Vargaftik, N. B. *Tables on thermophysical properties of liquids and gases*; Hemisphere Publ. Co.: Washington, 1975.